Luminosities and energies of e^+e^- collision data taken between $\sqrt{s}$=4.61 GeV and 4.95 GeV at BESIII*

M. Ablikim(麦迪娜)[1] M. N. Achasov[11,b] P. Adlarson[70] M. Albrecht[4] R. Aliberti[31] A. Amoroso[69A,69C] M. R. An(安美儒)[35] Q. An(安琪)[53,66] X. H. Bai(白旭红)[61] Y. Bai(白羽)[52] O. Bakina[32] Ferroli R. Baldini[26A] I. Balossino[27A,1] Y. Ban(班勇)[42,g] V. Batozskaya[1,40] D. Becker[31] K. Begzsuren[29] N. Berger[31] M. Bertani[26A] D. Bettoni[27A] F. Bianchi[69A,69C] J. Bloms[63] A. Bortone[69A,69C] I. Boyko[32] R. A. Briere[5] A. Brueggemann[63] H. Cai(蔡浩)[71] X. Cai(蔡啸)[1,53] A. Calcaterra[26A] G. F. Cao(曹国富)[1,58] N. Cao(曹宁)[1,58] S. A. Cetin[57A] J. F. Chang(常劲帆)[1,53] W. L. Chang(常万玲)[1,58] G. Chelkov[32,a] C. Chen(陈琛)[39] Chao Chen(陈超)[50] G. Chen(陈刚)[1] H. S. Chen(陈和生)[1,58] M. L. Chen(陈玛丽)[1,53] S. J. Chen(陈申见)[38] S. M. Chen(陈少敏)[56] T. Chen[1] X. R. Chen(陈旭荣)[28,58] X. T. Chen[1] Y. B. Chen(陈元柏)[1,53] Z. J. Chen(陈卓俊)[23,h] W. S. Cheng(成伟帅)[69C] X. Chu(初晓)[39] G. Cibinetto[27A] F. Cossio[69C] J. J. Cui(崔佳佳)[45] H. L. Dai(代洪亮)[1,53] J. P. Dai(代建平)[73] A. Dbeyssi[17] Boer R. E. de[4] D. Dedovich[32] Z. Y. Deng(邓子艳)[1] A. Denig[31] I. Denysenko[32] M. Destefanis[69A,69C] Mori F. De[69A,69C] Y. Ding(丁勇)[36] J. Dong(董静)[1,53] L. Y. Dong(董燎原)[1,58] M. Y. Dong(董明义)[1] X. Dong(董翔)[71] S. X. Du(杜书先)[75] P. Egorov[32,a] Y. L. Fan(范玉兰)[71] J. Fang(方建)[1,53] S. S. Fang(房双世)[1,58] W. X. Fang(方文兴)[1] Y. Fang(方易)[1] R. Farinelli[27A] L. Fava[69B,69C] F. Feldbauer[4] G. Felici[26A] C. Q. Feng(封常青)[53,66] J. H. Feng(冯俊华)[54] K Fischer[64] M. Fritsch[4] C. Fritzsch[63] C. D. Fu(傅成栋)[1] H. Gao(高涵)[58] Y. N. Gao(高原宁)[42,g] Yang Gao(高扬)[53,66] S. Garbolino[69C] I. Garzia[27A,27B] P. T. Ge(葛潘婷)[71] Z. W. Ge(葛振武)[38] C. Geng(耿聪)[54] E. M. Gersabeck[62] A Gilman[64] K. Goetzen[12] L. Gong(龚丽)[36] W. X. Gong(龚文煊)[1,53] W. Gradl[31] M. Greco[69A,69C] L. M. Gu(谷立民)[38] M. H. Gu(顾旻皓)[1,53] Y. T. Gu(顾运厅)[14] C. Y Guan(关春懿)[1,58] A. Q. Guo(郭爱强)[28,58] L. B. Guo(郭立波)[37] R. P. Guo(郭如盼)[44] Y. P. Guo(郭玉萍)[10,f] A. Guskov[32,a] T. T. Han(韩婷婷)[45] W. Y. Han(韩文颖)[35] X. Q. Hao(郝喜庆)[18] F. A. Harris[60] K. K. He(何凯凯)[50] K. L. He(何康林)[1,58] F. H. Heinsius[4] C. H. Heinz[31] Y. K. Heng(衡月昆)[1] C. Herold[55] M. Himmelreich[12,d] G. Y. Hou(侯国一)[1,58] Y. R. Hou(侯颖锐)[58] Z. L. Hou(侯治龙)[1] H. M. Hu(胡海明)[1,58] J. F. Hu[51,i] T. Hu(胡涛)[1] Y. Hu(胡誉)[1] G. S. Huang(黄光顺)[53,66] K. X. Huang(黄凯旋)[54] L. Q. Huang(黄麟钦)[67] L. Q. Huang(黄麟钦)[28,58] X. T. Huang(黄性涛)[45] Y. P. Huang(黄燕萍)[1] Z. Huang(黄震)[42,g] T. Hussain[68] N Hüsken[25,31] W. Imoehl[25] M. Irshad[53,66] J. Jackson[25] S. Jaeger[4] S. Janchiv[29] Q. Ji(纪全)[1] Q. P. Ji(姬清平)[18] X. B. Ji(季晓斌)[1,58] X. L. Ji(季筱璐)[1,53] Y. Y. Ji(吉钰瑶)[45] Z. K. Jia(贾泽坤)[53,66] H. B. Jiang(姜侯兵)[45] S. S. Jiang(姜赛赛)[35] X. S. Jiang(江晓山)[1] Y. Jiang[58] J. B. Jiao(焦健斌)[45] Z. Jiao(焦铮)[21] S. Jin(金山)[38] Y. Jin(金毅)[61] M. Q. Jing(荆茂强)[1,58] T. Johansson[70] N. Kalantar-Nayestanaki[59] X. S. Kang(康晓珅)[36] R. Kappert[59] B. C. Ke(柯百谦)[75] I. K. Keshk[4] A. Khoukaz[63] P. Kiese[31] R. Kiuchi[1] R. Kliemt[12] L. Koch[33] O. B. Kolcu[57A] B. Kopf[4] M. Kuemmel[4] M. Kuessner[4] A. Kupsc[40,70] W. Kühn[33]

Received 11 May 2022; Accepted 28 July 2022; Published online 6 September 2022

* Supported in part by National Key R&D Program of China (2020YFA0406400, 2020YFA0406300); National Natural Science Foundation of China (NSFC) (11635010, 11735014, 11805086, 11835012, 11935015, 11935016, 11935018, 11961141012, 12022510, 12025502, 12035009, 12035013, 12192260, 12192261, 12192262, 12192263, 12192264, 12192265); the Chinese Academy of Sciences (CAS) Large-Scale Scientific Facility Program; Joint Large-Scale Scientific Facility Funds of the NSFC and CAS (U1832207); CAS Key Research Program of Frontier Sciences (QYZDJ-SSW-SLH040); 100 Talents Program of CAS; Fundamental Research Funds for the Central Universities, Lanzhou University, University of Chinese Academy of Sciences; The Institute of Nuclear and Particle Physics (INPAC) and Shanghai Key Laboratory for Particle Physics and Cosmology; ERC (758462); European Union's Horizon 2020 research and innovation programme under Marie Sklodowska-Curie grant agreement (894790); German Research Foundation DFG (443159800), Collaborative Research Center CRC 1044, GRK 2149; Istituto Nazionale di Fisica Nucleare, Italy; Ministry of Development of Turkey (DPT2006K-120470); National Science and Technology fund; National Science Research and Innovation Fund (NSRF) via the Program Management Unit for Human Resources & Institutional Development, Research and Innovation (B16F640076); STFC (United Kingdom); Suranaree University of Technology (SUT), Thailand Science Research and Innovation (TSRI), and National Science Research and Innovation Fund (NSRF) (160355); The Royal Society, UK (DH140054, DH160214); The Swedish Research Council; U. S. Department of Energy (DE-FG02-05ER41374)

J. J. Lane[62] J. S. Lange[33] P. Larin[17] A. Lavania[24] L. Lavezzi[69A,69C] Z. H. Lei(雷祚弘)[53,66] H. Leithoff[31]
M. Lellmann[31] T. Lenz[31] C. Li(李翠)[43] C. Li(李聪)[39] C. H. Li(李春花)[35] Cheng Li(李澄)[53,66]
D. M. Li(李德民)[75] F. Li(李飞)[1,53] G. Li(李刚)[1] H. Li(李慧)[47] H. Li(李贺)[53,66] H. B. Li(李海波)[1,58]
H. J. Li(李惠静)[18] H. N. Li[51,i] J. Q. Li[4] J. S. Li(李静舒)[54] J. W. Li(李井文)[45] Ke Li(李科)[1] L. J. Li(李林健)[1]
L. K. Li(李龙科)[1] Lei Li(李蕾)[3] M. H. Li(李明浩)[39] P. R. Li(李培荣)[34,j,k] S. X. Li(李素娴)[10]
S. Y. Li(栗帅迎)[56] T. Li(李腾)[45] W. D. Li(李卫东)[1,58] W. G. Li(李卫国)[1] X. H. Li(李旭红)[53,66]
X. L. Li(李晓玲)[45] Xiaoyu Li(李晓宇)[1,58] H. Liang(梁昊)[53,66] H. Liang(梁浩)[1,58] H. Liang(梁浩)[30]
Y. F. Liang(梁勇飞)[49] Y. T. Liang(梁羽铁)[28,58] G. R. Liao(廖广睿)[13] L. Z. Liao(廖龙洲)[45] J. Libby[24]
A. Limphirat[55] C. X. Lin(林创新)[54] D. X. Lin(林德旭)[28,58] T. Lin[1] B. J. Liu(刘北江)[1] C. X. Liu(刘春秀)[1]
D. Liu[17,66] F. H. Liu(刘福虎)[48] Fang Liu(刘芳)[1] Feng Liu(刘峰)[6] G. M. Liu[51,i] H. Liu[34,j,k] H. B. Liu(刘宏邦)[14]
H. M. Liu(刘怀民)[1,58] Huanhuan Liu(刘欢欢)[1] Huihui Liu(刘汇慧)[19] J. B. Liu(刘建北)[53,66] J. L. Liu(刘佳俊)[67]
J. Y. Liu(刘晶译)[1,58] K. Liu(刘凯)[1] K. Y. Liu(刘魁勇)[36] Ke Liu(刘珂)[20] L. Liu(刘亮)[53,66] Lu Liu(刘露)[39]
M. H. Liu(刘美宏)[10,f] P. L. Liu(刘佩莲)[1] Q. Liu(刘倩)[58] S. B. Liu(刘树彬)[53,66] T. Liu(刘桐)[10,f]
W. K. Liu(刘维克)[39] W. M. Liu(刘卫民)[53,66] X. Liu(刘翔)[34,j,k] Y. Liu(刘英)[34,j,k] Y. B. Liu(刘玉斌)[39]
Z. A. Liu(刘振安)[1] Z. Q. Liu(刘智青)[45] X. C. Lou(娄辛丑)[1] F. X. Lu(卢飞翔)[54] H. J. Lu(吕海江)[21]
J. G. Lu(吕军光)[1,53] X. L. Lu(陆小玲)[1] Y. Lu(卢宇)[7] Y. P. Lu(卢云鹏)[1,53] Z. H. Lu[1] C. L. Luo(罗成林)[37]
M. X. Luo(罗民兴)[74] T. Luo(罗涛)[10,f] X. L. Luo(罗小兰)[1,53] X. R. Lyu(吕晓睿)[58] Y. F. Lyu(吕翌丰)[39]
F. C. Ma(马凤才)[36] H. L. Ma(马海龙)[1] L. L. Ma(马连良)[45] M. M. Ma(马明明)[1,58] Q. M. Ma(马秋梅)[1]
R. Q. Ma(马润秋)[1,58] R. T. Ma(马瑞廷)[58] X. Y. Ma(马骁妍)[1,53] Y. Ma(马尧)[42,g] F. E. Maas[17] M. Maggiora[69A,69C]
S. Maldaner[4] S. Malde[64] Q. A. Malik[68] A. Mangoni[26B] Y. J. Mao(冒亚军)[42,g] Z. P. Mao(毛泽普)[1]
S. Marcello[69A,69C] Z. X. Meng(孟召霞)[61] J. G. Messchendorp[59] G. Mezzadri[27A,1] H. Miao[1] T. J. Min(闵天觉)[38]
R. E. Mitchell[25] X. H. Mo(莫晓虎)[1] N. Yu. Muchnoi[11,b] Y. Nefedov[32] F. Nerling[17,d] I. B. Nikolaev[11,b]
Z. Ning(宁哲)[1,53] S. Nisar[9,l] Y. Niu(牛艳)[45] S. L. Olsen[58] Q. Ouyang(欧阳群)[1] S. Pacetti[26B,26C] X. Pan(潘祥)[10,f]
Y. Pan(潘越)[52] A. Pathak[30] M. Pelizaeus[4] H. P. Peng(彭海平)[53,66] K. Peters[12,d] J. L. Ping(平加伦)[37]
R. G. Ping(平荣刚)[1,58] S. Plura[31] S. Pogodin[32] V. Prasad[53,66] F. Z. Qi(齐法制)[1] H. Qi(齐航)[53,66]
H. R. Qi(漆红荣)[56] M. Qi(祁鸣)[38] T. Y. Qi(齐天钰)[10,f] S. Qian(钱森)[1,53] W. B. Qian(钱文斌)[58] Z. Qian(钱圳)[54]
C. F. Qiao(乔从丰)[58] J. J. Qin(秦佳佳)[67] L. Q. Qin(秦丽清)[13] X. P. Qin(覃潇平)[10,f] X. S. Qin(秦小帅)[45]
Z. H. Qin(秦中华)[1,53] J. F. Qiu(邱进发)[1] S. Q. Qu(屈三强)[56] K. H. Rashid[68] C. F. Redmer[31] K. J. Ren(任旷洁)[35]
A. Rivetti[69C] V. Rodin[59] M. Rolo[69C] G. Rong(荣刚)[1,58] Ch. Rosner[17] S. N. Ruan(阮氏宁)[39]
H. S. Sang(桑昊榆)[66] A. Sarantsev[32,c] Y. Schelhaas[31] C. Schnier[4] K. Schoenning[70] M. Scodeggio[27A,27B]
K. Y. Shan(尚科羽)[10,f] W. Shan(单葳)[22] X. Y. Shan(单心钰)[53,66] J. F. Shangguan(上官剑锋)[50]
L. G. Shao(邵立港)[1,58] M. Shao(邵明)[53,66] C. P. Shen(沈成平)[10,f] H. F. Shen(沈宏飞)[1,58] X. Y. Shen(沈肖雁)[1,58]
B. A. Shi(施伯安)[58] H. C. Shi(石煌超)[53,66] J. Y. Shi(石京燕)[1] q. q. Shi(石勤强)[50] R. S. Shi(师荣盛)[1,58]
X. Shi(史欣)[1,53] Shi X. D(师晓东)[53,66] J. J. Song(宋娇娇)[18] W. M. Song(宋维民)[1,30] Y. X. Song(宋昀轩)[42,g]
S. Sosio[69A,69C] S. Spataro[69A,69C] F. Stieler[31] K. X. Su(苏可馨)[71] P. P. Su(苏彭彭)[50] Y. J. Su(粟杨捷)[58]
G. X. Sun(孙功星)[1] H. Sun[58] H. K. Sun(孙浩凯)[1] J. F. Sun(孙俊峰)[18] L. Sun(孙亮)[71] S. S. Sun(孙胜森)[1,58]
T. Sun(孙童)[1,58] W. Y. Sun(孙文玉)[30] X Sun(孙翔)[23,h] Y. J. Sun(孙勇杰)[53,66] Y. Z. Sun(孙永昭)[1]
Z. T. Sun(孙振田)[45] Y. H. Tan(谭英华)[71] Y. X. Tan(谭雅星)[53,66] C. J. Tang(唐昌建)[49] G. Y. Tang(唐光毅)[1]
J. Tang(唐健)[54] L. Y Tao(陶璐燕)[67] Q. T. Tao(陶秋田)[23,h] M. Tat[64] J. X. Teng(滕佳秀)[53,66] V. Thoren[70]
W. H. Tian(田文辉)[47] Y. Tian(田野)[28,58] I. Uman[57B] B. Wang(王斌)[1] B. L. Wang(王滨龙)[58]
C. W. Wang(王成伟)[38] D. Y. Wang(王大勇)[42,g] F. Wang(王菲)[67] H. J. Wang(王泓鉴)[34,j,k] H. P. Wang(王宏鹏)[1,58]
K. Wang(王科)[1,53] L. L. Wang(王亮亮)[1] M. Wang(王萌)[45] M. Z. Wang(王梦真)[42,g] Meng Wang(王蒙)[1,58]
S. Wang[13] S. Wang(王顺)[10,f] T. Wang(王婷)[10,f] T. J. Wang(王腾蛟)[39] W. Wang(王为)[54] W. H. Wang(王文欢)[71]
W. P. Wang(王维平)[53,66] X. Wang(王轩)[42,g] X. F. Wang(王雄飞)[34,j,k] X. L. Wang(王小龙)[10,f] Y. Wang(王亦)[56]
Y. D. Wang(王雅迪)[41] Y. F. Wang(王贻芳)[1] Y. H. Wang(王英豪)[43] Y. Q. Wang(王雨晴)[1]
Yaqian Wang(王亚乾)[1,16] Z. Wang(王铮)[1,53] Z. Y. Wang(王至勇)[1,58] Ziyi Wang(王子一)[58] D. H. Wei(魏代会)[13]

F. Weidner[63] S. P. Wen(文硕频)[1] D. J. White[62] U. Wiedner[4] G. Wilkinson[64] M. Wolke[70] L. Wollenberg[4]
J. F. Wu(吴金飞)[1,58] L. H. Wu(伍灵慧)[1] L. J. Wu(吴连近)[1,58] X. Wu(吴潇)[10,f] X. H. Wu(伍雄浩)[30] Y. Wu[66]
Z. Wu(吴智)[1,53] L. Xia(夏磊)[53,66] T. Xiang(相腾)[42,g] D. Xiao(肖栋)[34,j,k] G. Y. Xiao(肖光延)[38] H. Xiao(肖浩)[10,f]
S. Y. Xiao(肖素玉)[1] Y. L. Xiao(肖云龙)[10,f] Z. J. Xiao(肖振军)[37] C. Xie(谢陈)[38] X. H. Xie(谢昕海)[42,g]
Y. Xie(谢勇)[45] Y. G. Xie(谢宇广)[1,53] Y. H. Xie(谢跃红)[6] Z. P. Xie(谢智鹏)[53,66] T. Y. Xing(邢天宇)[1,58]
C. F. Xu[1] C. J. Xu(许创杰)[54] G. F. Xu(许国发)[1] H. Y. Xu(许皓月)[61] Q. J. Xu(徐庆君)[15] X. P. Xu(徐新平)[50]
Y. C. Xu(胥英超)[58,76] Z. P. Xu(许泽鹏)[38] F. Yan(严芳)[10,f] L. Yan(严亮)[10,f] W. B. Yan(鄢文标)[53,66]
W. C. Yan(闫文成)[75] H. J. Yang(杨海军)[46,e] H. L. Yang(杨昊霖)[30] H. X. Yang(杨洪勋)[1] L. Yang(杨玲)[47]
S. L. Yang[58] Tao Yang(杨涛)[1] Y. F. Yang(杨艳芳)[39] Y. X. Yang(杨逸翔)[1,58] Yifan Yang(杨翊凡)[1,58]
M. Ye(叶梅)[1,53] M. H. Ye(叶铭汉)[8] J. H. Yin(殷俊昊)[1] Z. Y. You(尤郑昀)[54] B. X. Yu(俞伯祥)[1]
C. X. Yu(喻纯旭)[39] G. Yu(余刚)[1,58] T. Yu(于涛)[67] C. Z. Yuan(苑长征)[1,58] L. Yuan(袁丽)[2] S. C. Yuan[1]
X. Q. Yuan(袁晓庆)[1] Y. Yuan(袁野)[1,58] Z. Y. Yuan(袁朝阳)[54] C. X. Yue(岳崇兴)[35] A. A. Zafar[68]
F. R. Zeng(曾凡蕊)[45] X. Zeng(曾鑫)[6] Y. Zeng(曾云)[23,h] Y. H. Zhan(詹永华)[54] A. Q. Zhang(张安庆)[1]
B. L. Zhang[1] B. X. Zhang(张丙新)[1] D. H. Zhang(张丹昊)[39] G. Y. Zhang(张广义)[18] H. Zhang[66]
H. H. Zhang(张宏浩)[54] H. H. Zhang(张宏宏)[30] H. Y. Zhang(章红宇)[1,53] J. L. Zhang(张杰磊)[72]
J. Q. Zhang(张敬庆)[37] J. W. Zhang(张家文)[1] J. X. Zhang[34,j,k] J. Y. Zhang(张建勇)[1] J. Z. Zhang(张景芝)[1,58]
Jianyu Zhang(张剑宇)[1,58] Jiawei Zhang(张嘉伟)[1,58] L. M. Zhang(张黎明)[56] L. Q. Zhang(张丽青)[54]
Lei Zhang(张雷)[38] P. Zhang[1] Q. Y. Zhang(张秋岩)[35,75] Shuihan Zhang(张水涵)[1,58] Shulei Zhang(张书磊)[23,h]
X. D. Zhang(张小东)[41] X. M. Zhang[1] X. Y. Zhang(张学尧)[45] X. Y. Zhang(张旭颜)[50] Y. Zhang[64]
Y. T. Zhang(张亚腾)[75] Y. H. Zhang(张银鸿)[1,53] Yan Zhang(张言)[53,66] Yao Zhang(张瑶)[1] Z. H. Zhang[1]
Z. Y. Zhang(张振宇)[71] Z. Y. Zhang(张子羽)[39] G. Zhao(赵光)[1] J. Zhao(赵静)[35] J. Y. Zhao(赵静宜)[1,58]
J. Z. Zhao(赵京周)[1,53] Lei Zhao(赵雷)[53,66] Ling Zhao(赵玲)[1] M. G. Zhao(赵明刚)[39] Q. Zhao(赵强)[1]
S. J. Zhao(赵书俊)[75] Y. B. Zhao(赵豫斌)[1,53] Y. X. Zhao(赵宇翔)[28,58] Z. G. Zhao(赵政国)[53,66] A. Zhemchugov[32,a]
B. Zheng(郑波)[67] J. P. Zheng(郑建平)[1,53] Y. H. Zheng(郑阳恒)[58] B. Zhong(钟彬)[37] C. Zhong(钟翠)[67]
X. Zhong(钟鑫)[54] H. Zhou(周航)[45] L. P. Zhou(周利鹏)[1,58] X. Zhou(周详)[71] X. K. Zhou(周晓康)[58]
X. R. Zhou(周小蓉)[53,66] X. Y. Zhou(周兴玉)[35] Y. Z. Zhou(周祎卓)[10,f] J. Zhu(朱江)[39] K. Zhu(朱凯)[1]
K. J. Zhu(朱科军)[1] L. X. Zhu(朱琳萱)[58] S. H. Zhu(朱世海)[65] S. Q. Zhu(朱仕强)[38] T. J. Zhu(朱腾蛟)[72]
W. J. Zhu(朱文静)[10,f] Y. C. Zhu(朱莹春)[53,66] Z. A. Zhu(朱自安)[1,58] B. S. Zou(邹冰松)[1] J. H. Zou(邹佳恒)[1]

(BESIII Collaboration)

[1]Institute of High Energy Physics, Beijing 100049, China
[2]Beihang University, Beijing 100191, China
[3]Beijing Institute of Petrochemical Technology, Beijing 102617, China
[4]Bochum Ruhr-University, D-44780 Bochum, Germany
[5]Carnegie Mellon University, Pittsburgh, Pennsylvania 15213, USA
[6]Central China Normal University, Wuhan 430079, China
[7]Central South University, Changsha 410083, China
[8]China Center of Advanced Science and Technology, Beijing 100190, China
[9]COMSATS University Islamabad, Lahore Campus, Defence Road, Off Raiwind Road, 54000 Lahore, Pakistan
[10]Fudan University, Shanghai 200433, China
[11]G.I. Budker Institute of Nuclear Physics SB RAS (BINP), Novosibirsk 630090, Russia
[12]GSI Helmholtzcentre for Heavy Ion Research GmbH, D-64291 Darmstadt, Germany
[13]Guangxi Normal University, Guilin 541004, China
[14]Guangxi University, Nanning 530004, China
[15]Hangzhou Normal University, Hangzhou 310036, China
[16]Hebei University, Baoding 071002, China
[17]Helmholtz Institute Mainz, Staudinger Weg 18, D-55099 Mainz, Germany
[18]Henan Normal University, Xinxiang 453007, China
[19]Henan University of Science and Technology, Luoyang 471003, China
[20]Henan University of Technology, Zhengzhou 450001, China
[21]Huangshan College, Huangshan 245000, China
[22]Hunan Normal University, Changsha 410081, China
[23]Hunan University, Changsha 410082, China
[24]Indian Institute of Technology Madras, Chennai 600036, India
[25]Indiana University, Bloomington, Indiana 47405, USA

[26A]INFN Laboratori Nazionali di Frascati, I-00044, Frascati, Italy
[26B]INFN Sezione di Perugia, I-06100, Perugia, Italy
[26C]University of Perugia, I-06100, Perugia, Italy
[27A]INFN Sezione di Ferrara, I-44122, Ferrara, Italy
[27B]University of Ferrara, I-44122, Ferrara, Italy
[28]Institute of Modern Physics, Lanzhou 730000, China
[29]Institute of Physics and Technology, Peace Avenue 54B, Ulaanbaatar 13330, Mongolia
[30]Jilin University, Changchun 130012, China
[31]Johannes Gutenberg University of Mainz, Johann-Joachim-Becher-Weg 45, D-55099 Mainz, Germany
[32]Joint Institute for Nuclear Research, 141980 Dubna, Moscow region, Russia
[33]Justus-Liebig-Universitaet Giessen, II. Physikalisches Institut, Heinrich-Buff-Ring 16, D-35392 Giessen, Germany
[34]Lanzhou University, Lanzhou 730000, China
[35]Liaoning Normal University, Dalian 116029, China
[36]Liaoning University, Shenyang 110036, China
[37]Nanjing Normal University, Nanjing 210023, China
[38]Nanjing University, Nanjing 210093, China
[39]Nankai University, Tianjin 300071, China
[40]National Centre for Nuclear Research, Warsaw 02-093, Poland
[41]North China Electric Power University, Beijing 102206, China
[42]Peking University, Beijing 100871, China
[43]Qufu Normal University, Qufu 273165, China
[44]Shandong Normal University, Jinan 250014, China
[45]Shandong University, Jinan 250100, China
[46]Shanghai Jiao Tong University, Shanghai 200240, China
[47]Shanxi Normal University, Linfen 041004, China
[48]Shanxi University, Taiyuan 030006, China
[49]Sichuan University, Chengdu 610064, China
[50]Soochow University, Suzhou 215006, China
[51]South China Normal University, Guangzhou 510006, China
[52]Southeast University, Nanjing 211100, China
[53]State Key Laboratory of Particle Detection and Electronics, Beijing 100049, Hefei 230026, China
[54]Sun Yat-Sen University, Guangzhou 510275, China
[55]Suranaree University of Technology, University Avenue 111, Nakhon Ratchasima 30000, Thailand
[56]Tsinghua University, Beijing 100084, China
[57A]Istinye University, 34010, Istanbul, Turkey
[57B]Near East University, Nicosia, North Cyprus, Mersin 10, Turkey
[58]University of Chinese Academy of Sciences, Beijing 100049, China
[59]University of Groningen, NL-9747 AA Groningen, The Netherlands
[60]University of Hawaii, Honolulu, Hawaii 96822, USA
[61]University of Jinan, Jinan 250022, China
[62]University of Manchester, Oxford Road, Manchester, M13 9PL, United Kingdom
[63]University of Muenster, Wilhelm-Klemm-Strasse 9, 48149 Muenster, Germany
[64]University of Oxford, Keble Road, Oxford OX13RH, United Kingdom
[65]University of Science and Technology Liaoning, Anshan 114051, China
[66]University of Science and Technology of China, Hefei 230026, China
[67]University of South China, Hengyang 421001, China
[68]University of the Punjab, Lahore-54590, Pakistan
[69A]University of Turin, I-10125, Turin, Italy
[69B]University of Eastern Piedmont, I-15121, Alessandria, Italy
[69C]INFN, I-10125, Turin, Italy
[70]Uppsala University, Box 516, SE-75120 Uppsala, Sweden
[71]Wuhan University, Wuhan 430072, China
[72]Xinyang Normal University, Xinyang 464000, China
[73]Yunnan University, Kunming 650500, China
[74]Zhejiang University, Hangzhou 310027, China
[75]Zhengzhou University, Zhengzhou 450001, China
[76]Yantai University, Yantai 264005, China
[a]Also at the Moscow Institute of Physics and Technology, Moscow 141700, Russia
[b]Also at the Novosibirsk State University, Novosibirsk, 630090, Russia
[c]Also at the NRC "Kurchatov Institute", PNPI, 188300, Gatchina, Russia
[d]Also at Goethe University Frankfurt, 60323 Frankfurt am Main, Germany
[e]Also at Key Laboratory for Particle Physics, Astrophysics and Cosmology, Ministry of Education; Shanghai Key Laboratory for Particle Physics and Cosmology; Institute of Nuclear and Particle Physics, Shanghai 200240, China
[f]Also at Key Laboratory of Nuclear Physics and Ion-beam Application (MOE) and Institute of Modern Physics, Fudan University, Shanghai 200443, China
[g]Also at State Key Laboratory of Nuclear Physics and Technology, Peking University, Beijing 100871, China
[h]Also at School of Physics and Electronics, Hunan University, Changsha 410082, China
[i]Also at Guangdong Provincial Key Laboratory of Nuclear Science, Institute of Quantum Matter, South China Normal University,

Guangzhou 510006, China
[j]Also at Frontiers Science Center for Rare Isotopes, Lanzhou University, Lanzhou 730000, China
[k]Also at Lanzhou Center for Theoretical Physics, Lanzhou University, Lanzhou 730000, China
[l]Also at the Department of Mathematical Sciences, IBA, Karachi, Pakistan

Abstract: From December 2019 to June 2021, the BESIII experiment collected approximately 5.85 fb^{-1} of data at center-of-mass energies between 4.61 and 4.95 GeV. This is the highest collision energy BEPCII has reached to date. The accumulated e^+e^- annihilation data samples are useful for studying charmonium(-like) states and charmed-hadron decays. By adopting a novel method of analyzing the production of $\Lambda_c^+\bar{\Lambda}_c^-$ pairs in e^+e^- annihilation, the center-of-mass energies are measured with a precision of ~0.6 MeV. Integrated luminosities are measured with a precision of better than 1% by analyzing the events of large-angle Bhabha scattering. These measurements provide important inputs to analyses based on these data samples.

Keywords: luminosity, center-of-mass energy, BESIII detector

DOI: 10.1088/1674-1137/ac84cc

I. INTRODUCTION

In 2020, BEPCII implemented an energy upgrade project and increased the maximum center-of-mass energy from 4.61 to 4.95 GeV. During the data-taking years of 2020 and 2021, the BESIII experiment collected e^+e^- annihilation data at 12 center-of-mass energy ($E_{\rm cms}$) points between 4.61 and 4.95 GeV. In this energy region, a few charmonium(-like) states can be produced, such as Y(4630) and Y(4660) [1–5], which are potential candidates for multi-quark states other than charmonium states [6]. More strikingly, at 4.68 GeV, the BESIII experiment observed the first candidate for a charged hidden-charm tetraquark with strangeness, $Z_{cs}(3985)^+$ [7]. Note that charge conjugation is always implied. In addition, $\Lambda_c^+\bar{\Lambda}_c^-$ pair-production is open in this energy region. This provides many opportunities for precise measurements of the properties of the lightest charmed baryon Λ_c^+, with threshold production and quantum coherence of the accumulated $\Lambda_c^+\bar{\Lambda}_c^-$ pairs. In 2014, the BESIII experiment collected 567 pb^{-1} of e^+e^- annihilation data at 4.599 GeV, which led to many pioneering measurements [8–14]. Approximately ten times more $\Lambda_c^+\bar{\Lambda}_c^-$ pair events are expected to be contained in all data taken above 4.6 GeV, which provides great potential to improve our knowledge of the strong and weak interactions in the charm sector [15]. The $E_{\rm cms}$ and integrated luminosities of these data samples are important inputs for analyses using these data samples.

In this paper, we present measurements of $E_{\rm cms}$ and integrated luminosity for data samples at various energy points, as listed in Table 1. The Beam Energy Measurement System (BEMS) [16], which was installed in 2008, is designed to precisely measure the beam energy based

Table 1. Numerical results for the center-of-mass energy $E_{\rm cms}$, the integrated luminosity measured with the Bhabha process $\mathscr{L}_{\rm Bhabha}$, the integrated luminosity measured with the di-photon process $\mathscr{L}_{\rm di-photon}$, and their ratio for all data samples. For the $E_{\rm cms}$ and $\mathscr{L}_{\rm Bhabha}$ measurements, the first uncertainty is statistical and the second is systematic. For the $\mathscr{L}_{\rm di-photon}$ measurement, only statistical uncertainties are presented. For the ratio of $\mathscr{L}_{\rm di-photon}$ to $\mathscr{L}_{\rm Bhabha}$, all presented uncertainties are considered.

Sample	$E_{\rm cms}$/MeV	$\mathscr{L}_{\rm Bhabha}$/pb^{-1}	$\mathscr{L}_{\rm di-photon}$/pb^{-1}	Ratio (%)
4610	4611.86±0.12±0.30	103.65±0.05±0.55	103.37±0.13	99.73±0.59
4620	4628.00±0.06±0.32	521.53±0.11±2.76	520.17±0.28	99.74±0.55
4640	4640.91±0.06±0.38	551.65±0.12±2.92	550.67±0.29	99.82±0.55
4660	4661.24±0.06±0.29	529.43±0.12±2.81	527.53±0.29	99.64±0.55
4680	4681.92±0.08±0.29	1667.39±0.21±8.84	1665.88±0.51	99.91±0.54
4700	4698.82±0.10±0.36	535.54±0.12±2.84	533.66±0.29	99.64±0.55
4740	4739.70±0.20±0.30	163.87±0.07±0.87	165.08±0.16	100.74±0.58
4750	4750.05±0.12±0.29	366.55±0.10±1.94	367.57±0.24	100.28±0.56
4780	4780.54±0.12±0.30	511.47±0.12±2.71	512.03±0.29	100.11±0.55
4840	4843.07±0.20±0.31	525.16±0.12±2.78	526.01±0.30	100.16±0.55
4920	4918.02±0.34±0.34	207.82±0.08±1.10	208.09±0.19	100.13±0.57
4950	4950.93±0.36±0.38	159.28±0.07±0.84	159.85±0.17	100.36±0.58

on the energies of Compton back-scattered photons. However, the working range of BEMS is below 4 GeV, which implies that the measurement of $E_{\rm cms}$ for data samples involved in this paper must be performed offline. A novel method of using $e^+e^- \to \Lambda_c^+\bar{\Lambda}_c^-$ events is adopted, which was discussed in the energy measurement for $\psi(3770)$ data at BESIII [17]. In the luminosity measurement, the Bhabha scattering process $e^+e^- \to (\gamma)\, e^+e^-$ is used, benefiting from its clear signature and large production cross section, which allow for a negligible statistical uncertainty and relatively small systematic uncertainty. A cross check of the luminosity results is performed by analyzing the di-photon process $e^+e^- \to (\gamma)\, \gamma\gamma$.

II. BESIII DETECTOR AND MC SIMULATIONS

The BESIII detector [18] records symmetric e^+e^- collisions provided by the BEPCII storage ring [19], which operates at center-of-mass energies ranging from 2.0 to 4.95 GeV. BESIII has collected large data samples in this energy region [20]. The cylindrical core of the BESIII detector covers 93% of the full solid angle and consists of a helium-based multilayer drift chamber (MDC), plastic scintillator time-of-flight system (TOF), and CsI(Tl) electromagnetic calorimeter (EMC), which are all enclosed in a superconducting solenoidal magnet providing a 1.0 T magnetic field. The solenoid is supported by an octagonal flux-return yoke with resistive plate counter muon identification modules interleaved with steel. The charged-particle momentum resolution at 1 GeV/c is 0.5%, and the dE/dx resolution is 6% for electrons from Bhabha scattering. The EMC measures photon energies with a resolution of 2.5% (5%) at 1 GeV in the barrel (end cap) region. The time resolution in the TOF barrel region is 68 ps, whereas that in the end cap region is 60 ps [21–23].

Simulated samples produced with a Geant4-based [24] Monte Carlo (MC) package, which includes a geometric description of the BESIII detector and detector response, are used to determine detection efficiencies and estimate backgrounds. The simulation models the beam energy spread and initial state radiation (ISR) in the e^+e^- annihilations with the generator KKMC [25, 26]. The inclusive MC sample includes the production of the process $\Lambda_c^+\bar{\Lambda}_c^-$ using the Born cross section line shape measured by BESIII, open charm processes, the ISR production of vector charmonium(-like) states, and the continuum processes incorporated in KKMC [25, 26]. The known decay modes are modeled with EVTGEN [27, 28] using branching fractions taken from the Particle Data Group (PDG) [29], and the remaining unknown charmonium decays are modeled with LUNDCHARM [30, 31]. Final state radiation (FSR) from charged final state particles is incorporated using PHOTOS [32].

III. MEASUREMENT OF CENTER-OF-MASS ENERGIES

In the process $e^+e^- \to \Lambda_c^+\bar{\Lambda}_c^-$, each Λ_c^+ ($\bar{\Lambda}_c^-$) baryon carries half the energy of $E_{\rm cms}$. Hence, $E_{\rm cms}$ is obtained from the calibrated beam energy E_{Λ_c} using the reconstructed mass of one Λ_c with the following equations:

$$\begin{aligned} E_{\rm cms} &= 2E_{\Lambda_c}, \\ E_{\Lambda_c}^2 &= E_0^2 + m_{\Lambda_c}^2 c^4 - M_{\rm BC}^2 c^4. \end{aligned} \tag{1}$$

Here, E_0 is the uncalibrated beam energy, with input values of 2306, 2313, 2320, 2330, 2340, 2350, 2370, 2375, 2390, 2420, 2457, and 2473 MeV for the beam energies of 12 different energy points, and m_{Λ_c} is the known Λ_c mass of 2286.46 ± 0.14 MeV/c^2 [29, 33]. $M_{\rm BC}$ is the fitted peak position of the beam-constrained mass of the Λ_c baryon calculated using $M_{\rm BC}c^2 = \sqrt{E_0^2 - p_{\Lambda_c}^2 c^2}$, where p_{Λ_c} is the momentum of the Λ_c measured in the center-of-mass system of the e^+e^- collision. Essentially, Eq. (1) is equivalent to $E_{\Lambda_c}^2 = p_{\Lambda_c}^2 c^2 + m_{\Lambda_c}^2 c^4$. The distributions of $M_{\rm BC}$, instead of p_{Λ_c}, are fitted because $M_{\rm BC}$ has better resolution and its fit quality is more easily controlled. According to the above analysis, we expect the calibrated beam energy E_{Λ_c} to be stable when different E_0 are used, which is well verified by both real data and MC simulations.

To perform this measurement, we use the partial reconstruction method, and only one Λ_c^+ is reconstructed for which the $\Lambda_c^+ \to pK^-\pi^+$ channel is used because of its relatively large decay rate and low background contamination. Each charged track must satisfy the following criteria: The distance of the closest approach of every charged track to the e^+e^- interaction point (IP) must be within 10 cm along the beam direction and within 1 cm on the plane perpendicular to the beam direction. The polar angle θ between the direction of a charged track and that of the positron beam must satisfy $|\cos\theta| < 0.93$ for an effective measurement in the active volume of the MDC. The dE/dx information recorded by the MDC and time-of-flight information measured by the TOF are combined to calculate particle identification (PID) probabilities for various particle hypotheses. Tracks are identified as protons if their PID probabilities ($\mathcal{P}$) satisfy $\mathcal{P}(p) > \mathcal{P}(K)$ and $\mathcal{P}(p) > \mathcal{P}(\pi)$, whereas charged kaons and pions are identified using $\mathcal{P}(K) > \mathcal{P}(\pi)$ and $\mathcal{P}(\pi) > \mathcal{P}(K)$, respectively. All $pK^-\pi^+$ combinations in one event are kept for further study. In the fit to the $M_{\rm BC}$ distributions, the signals are described by the Bukin function [34], and the backgrounds are described by a linear function. The fit result of the 4680 MeV data sample is shown in Fig. 1.

To validate the analysis method, an input and output (I/O) check based on the inclusive MC simulation is performed. Systematic shifts (0.09 ~ 0.25 MeV) are noticed

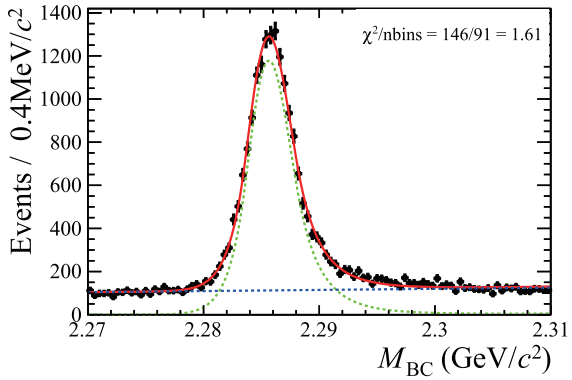

Fig. 1. (color online) Fit to the $M_{\rm BC}$ distribution for $\Lambda_c^+ \to pK^-\pi^+$ candidates from the 4680 MeV data sample. The dotted green line is the fitted signal, and the dotted blue line is the fitted background. The black dots with error bars are data, and the red line is the sum of fit functions.

between the measured beam energies and the true simulated input values, mainly due to the ISR effect. The shifts at different energy points are considered as individual correction factors. The final values of the determined $E_{\rm cms}$ are listed in Table 1.

The systematic uncertainty on the $E_{\rm cms}$ measurement originates mainly from the uncertainty on the Λ_c mass quoted from the PDG, which is 0.28 MeV (twice the uncertainty on the Λ_c PDG mass). Other small uncertainties are due to the $M_{\rm BC}$ fit range and ISR correction. For the fit range, we vary the fit boundary and repeat the $M_{\rm BC}$ fit. The maximum relative changes of $E_{\rm cms}$ are taken as systematic uncertainties.

For ISR correction, we consider the cross section line shape and the influence of the background. An alternative cross section line shape is first obtained by varying the measured Born cross section line shape of the $e^+e^- \to \Lambda_c^+\bar{\Lambda}_c^-$ process within uncertainties. The alternative and nominal line shape are used to generate signal MC samples of the process $e^+e^- \to \Lambda_c^+\bar{\Lambda}_c^-$, where one Λ_c decays to $pK\pi$, and the other Λ_c decays inclusively, and then the I/O procedure is repeated to obtain the ISR correction factors. The differences in the ISR correction factors are regarded as systematic uncertainties. To consider the potential effect of background simulation, the difference in ISR correction between the signal MC sample and the inclusive MC sample is regarded as a systematic uncertainty.

For the signal and background shapes, the uncertainties are negligible based on MC simulation studies. A summary of systematic uncertainties is given in Table 2. For each energy point, the total systematic uncertainty is taken as the quadrature sum of each item.

We validate the energy measurements to the 12 data samples using the $e^+e^- \to D^+D^{*-}$ process, where D^+ is reconstructed via $D^+ \to K^-\pi^+\pi^+$. The recoil mass ofD^+, RM_{D^+}, is defined as

$$RM_{D^+} = \sqrt{(E_{\rm cms} - E_{D^+})^2/c^4 - (\vec{p}_{\rm cms} - \vec{p}_{D^+})^2/c^2}, \quad (2)$$

where E_{D^+} ($\vec{p}_{D^+}$) is the energy (momentum) of the reconstructed D^+. The total energy (momentum) of the initial e^+e^- system, $E_{\rm cms}$ ($\vec{p}_{\rm cms}$), is input according to our measurement. The peak values of the RM_{D^+} distributions correspond to the known mass of D^{*-} [29]. To improve the mass resolution [35], the variable $RM_{D^+} + M_{D^+} - m_{D^+}$ is adopted to represent the D^+ recoil mass spectrum, where M_{D^+} is the D^+ invariant mass, and m_{D^+} is the known D^+ mass [29]. The Bukin function is used to fit the $RM_{D^+} + M_{D^+} - m_{D^+}$ distribution to obtain the peak mass position, in which the tail shapes in the signal function are fixed according to the MC simulation of the process $e^+e^- \to D^+D^{*-}$. Following the same procedure used for

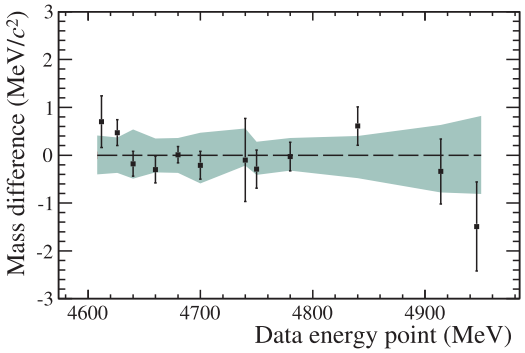

Fig. 2. (color online) Difference between the measured D^{*-} mass, using the validation sample of $e^+e^- \to D^+D^{*-}$, and the known D^{*-} mass at each energy point [29]. The points with error bars are from data, and the green band is the uncertainty due to that of the $E_{\rm cms}$ value.

Table 2. Systematic uncertainties on the $E_{\rm cms}$ measurement (in MeV). For each energy point, the total systematic uncertainty corresponds to the quadrature sum of each item.

Source	Sample											
	4610	4620	4640	4660	4680	4700	4740	4750	4780	4840	4920	4950
PDG mass	0.28	0.28	0.28	0.28	0.28	0.28	0.28	0.28	0.28	0.28	0.28	0.28
Fit range	0.04	0.14	0.22	0.04	0.04	0.14	0.04	0.04	0.04	0.02	0.17	0.24
ISR correction	0.10	0.06	0.13	0.07	0.06	0.17	0.11	0.04	0.09	0.13	0.09	0.08
Total	0.30	0.32	0.38	0.29	0.29	0.36	0.30	0.29	0.30	0.31	0.34	0.38

ISR correction in the nominal analysis, the measured mass of D^{*-} in the validation sample is consistent with the known D^{*-} mass [29]. Figure 2 shows the mass difference at each energy point, which is consistent with zero and hence validates the measured center-of-mass energies.

IV. MEASUREMENT OF INTEGRATED LUMINOSITIES

The integrated luminosity of the data sample is determined using

$$\mathscr{L} = \frac{N^{\rm obs}_{e^+e^-\to X}}{\sigma^{\rm obs}_{e^+e^-\to X}\times\epsilon_{e^+e^-\to X}}, \tag{3}$$

where X denotes any specific final state produced in e^+e^- annihilations, $N^{\rm obs}_{e^+e^-\to X}$ is the observed yield for the $e^+e^-\to X$ process, $\mathscr{L}$ is the integrated luminosity for data, and $\sigma^{\rm obs}_{e^+e^-\to X}$ is the visible cross section. Here, the Bhabha process $(e^+e^-\to(\gamma)e^+e^-)$ is analyzed in the nominal method, and the di-photon $e^+e^-\to(\gamma)\,\gamma\gamma$ process serves as a cross check channel. The observed cross sections for the two processes are provided by the BabaYaga@NLO generator [36] with 0.1% precision. The configuration parameters for the BabaYaga@NLO generator used in generating Bhabha events are listed in Table 3.

The criteria used to select Bhabha candidates include the following: We require only two oppositely charged tracks (nCharged) detected in the MDC that satisfy $|\cos\theta|<0.8$, and the distance requirement of the closest approach of each charged track to the IP is the same as described in Section III. Figure 3 shows the distributions of momentum, polar angle $\cos\theta$, and azimuthal angle ϕ for the electron and positron tracks measured in the MDC in the data and signal MC samples. Good consistency between data and MC simulation is shown. The momentum of each track must be larger than 2 GeV/c to reject backgrounds from hadronic processes. In addition, to suppress the backgrounds from di-photon process, $|\Delta\phi^{\rm EMC}|$ must be in the range $[5^\circ, 40^\circ]$, where $\Delta\phi^{\rm EMC} = |\phi^{\rm EMC}_1-\phi^{\rm EMC}_2|-180^\circ$, and $\phi^{\rm EMC}_{1,2}$ are the azimuthal angles of the two clusters produced by the electron and positron in the EMC in the center-of-mass frame.

Table 3. Configuration of the BabaYaga@NLO generator used for simulating Bhabha events.

Parameter	Value
$E_{\rm cms}$	Refer to Table 1
Beam energy spread	1.58 MeV
MinThetaAngle	20°
MaxThetaAngle	160°
Maximum Acollinearity	180°
NSearch	4000000
RunningAlpha	1
Number of photon	−1

Figure 4 shows the two-dimensional $E^{\rm EMC}$ distributions of e^+ and e^- in Bhabha candidate events, where $E^{\rm EMC}$ is the output of the deposited energies of clusters in the EMC. Owing to the unexpected saturation effect [37] from a small fraction of EMC electronic readouts, $E^{\rm EMC}$ of the electron and positron becomes underestimated and distributes around 0.4 GeV, which is significantly less than the expected energies. As shown in Fig. 4(a), a fraction (2) of the electron or positron tracks, depending on the track momentum, is influenced by the EMC saturation effect. To evaluate the relative size of this effect, the sample is divided into two categories: NORMAL SAMPLE ($E^{\rm EMC}(e^+)>1$ GeV and $E^{\rm EMC}(e^-)>1$ GeV) without saturated e^+e^- EMC clusters, and SATURATION SAMPLE ($E^{\rm EMC}(e^+)<1$ GeV or $E^{\rm EMC}(e^-)<1$ GeV) with at least one saturated e^+ or e^- EMC cluster. However, as shown in Fig. 4(b), MC simulations do not reflect the saturation effect. To obtain the total signal yields that correctly match the MC-determined efficiency, the signal yields in both the NORMAL SAMPLE and SATURATION SAMPLE are included.

For the NORMAL SAMPLE, backgrounds are negligible compared to the statistics of the signal yields. This is validated using the background MC sample, which contains the inclusive MC sample and all QED events except the Bhabha signal, as shown in Fig. 4(c). Hence, the survived NORMAL SAMPLE is taken as the signal. For the SATURATION SAMPLE, a portion of the background originates from the dimuon process $e^+e^-\to\mu^+\mu^-$, as indicated in Fig. 4(c). To extract the signal yields, the normalized pulse height, $PH_{\rm norm}$, from the specific ionization energy lost by the charged track in the MDC is adopted to distinguish Bhabha events from the dimuon backgrounds. Figure 5 shows the fit to the $PH_{\rm norm}$ distribution, where the signals peak at approximately 1.0 for the electron, and the dimuon backgrounds peak at approximately 0.86. In the fit, the shape of the electron signals is modeled using the electron sample in the NORMAL SAMPLE, and the muon shape is taken from the control sample of the dimuon process, where the penetration depth of the dimuon tracks in the muon counter must be larger than 10 cm and is implemented for data in the background region ($E^{\rm EMC}(e^+)<1$ GeV and $E^{\rm EMC}(e^-)<1$ GeV) in Fig. 4(a). The fitted yields of the Bhabha process are taken as signals in the SATURATION SAMPLE.

The sum of the signal yields in the NORMAL SAMPLE and SATURATION SAMPLE is taken as the total yield of the Bhabha events. The detection efficiency is estimated using the Bhabha MC samples, and the ob-

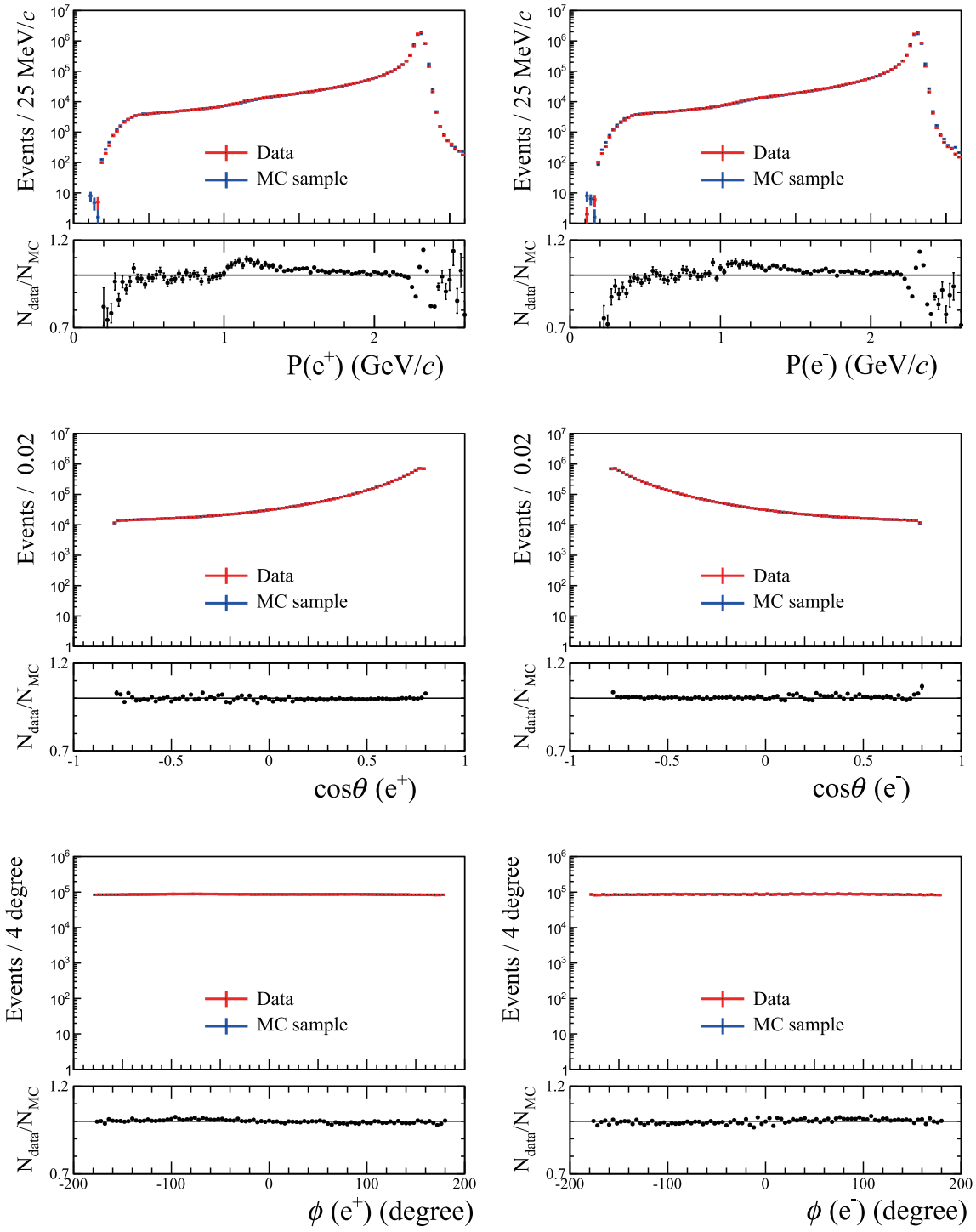

Fig. 3. (color online) Comparisons between the data and MC samples at the 4620 MeV energy point for the momentum (top), $\cos\theta$ (middle), and ϕ (bottom) distributions of e^+ (left) and e^- (right) in Bhabha events. $N_{\rm data}/N_{\rm MC}$ is the ratio of the data and MC samples. The red points with error bars are data, and the blue points are MC samples. The sizes of the MC samples are normalized to those in data. Except for the variable to be shown, all other requirements used in event selection are applied. Although the comparison shows inconsistency in the high momentum region of the momentum spectrum, this would not have a significant effect on the final results.

served Bhabha cross section is calculated with the BabaYaga@NLO generator. Therefore, the integrated luminosity of the data sample is calculated using Eq. (3), and the corresponding results for the 12 energy points are given in Table 1. The statistical precision of the measured luminosity is better than 0.05% at each energy point.

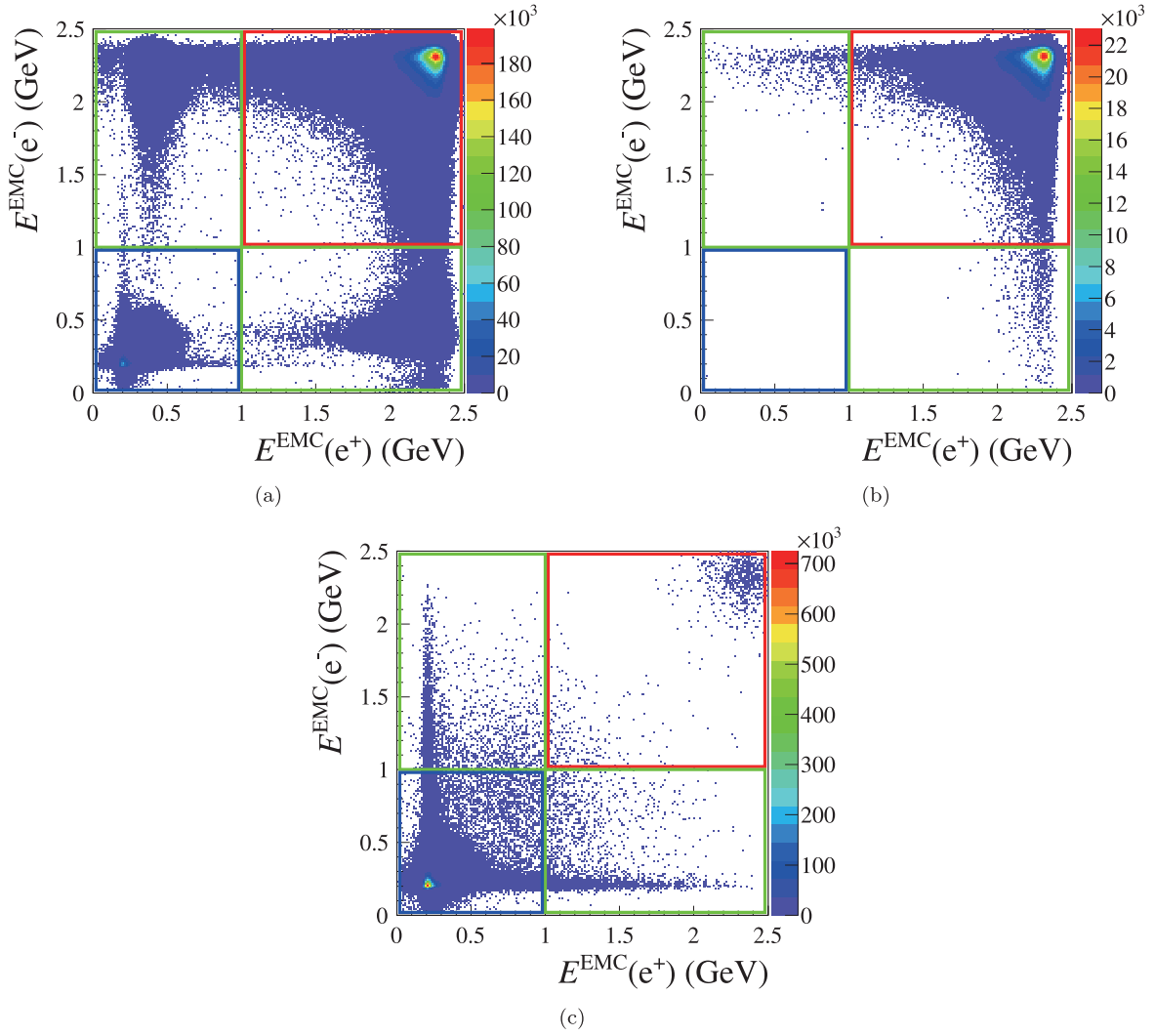

Fig. 4. (color online) Two-dimensional distributions of $E^{EMC}(e^-)$ versus $E^{EMC}(e^+)$ in data (a), the Bhabha MC sample (b), and background MC samples (c) for the 4620 MeV energy point. Three kinematic regions are presented: the red square region [$E^{EMC}(e^+) > 1$ GeV and $E^{EMC}(e^-) > 1$ GeV] for the NORMAL SAMPLE, and the remaining regions for the SATURATION SAMPLE. The dimuon backgrounds are concentrated in the blue square [$E^{EMC}(e^+) < 1$ GeV and $E^{EMC}(e^-) < 1$ GeV], as shown in plot (c).

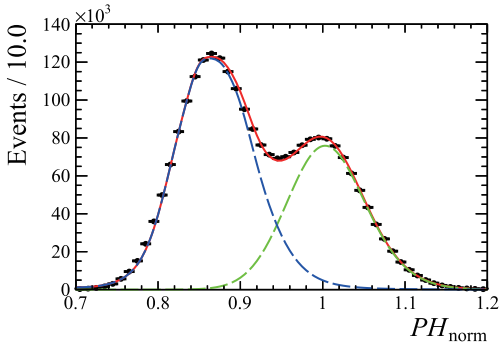

Fig. 5. (color online) Fit to the PH_{norm} distribution in the SATURATION SAMPLE from the 4620 MeV data sample. The black dots with error bars are data, the red line is the total fit, the long dashed blue line is background dominated by the dimuon process, and the dashed green line represents saturation events.

Table 4. Systematic uncertainties on the luminosity measurement. The total systematic uncertainty corresponds to the quadrature sum of each item.

Source	Uncertainty (%)
Tracking efficiency	0.30
nCharged requirement	0.10
Momentum requirement	0.18
$\cos\theta$ requirement	0.30
Saturation events	0.20
BabaYaga@NLO generator	0.10
MC statistics	0.05
Cross section	0.09
Total	0.53

Sources of systematic uncertainties in the luminosity measurement are summarized in Table 4. For the 12 energy points, common systematic uncertainties are assigned. Details are discussed below.

High momentum electron samples are selected to study the systematic uncertainties due to tracking, the nCharged requirement, the momentum requirement, and the $\cos\theta$ requirement. We select one e^+ with a momentum larger than 2 GeV/c and $E^{\rm EMC}(e^+)$ greater than 1 GeV as the positron candidate from the Bhabha process and take the recoil e^- as the control sample to study the efficiency of the selection criteria. The relative efficiency difference between the control sample and Bhabha MC sample is regarded as the systematic uncertainty.

For estimation of the signal yields, the main systematic issue is in the extraction of the signal yields in the SATURATION SAMPLE. As a check, a different method of counting the number of survived events is adopted after removing the dimuon backgrounds by discarding events in the regions $E^{\rm EMC}(e^+) < 1$ GeV and $E^{\rm EMC}(e^-) < 1$ GeV. In the remaining events of the SATURATION SAMPLE, there is a small fraction of backgrounds (approximately 0.50%), which is neglected. The resultant luminosity differs from the nominal result by 0.20%, which is taken as the systematic uncertainty.

For the BabaYaga@NLO generator, the theoretical uncertainty on the cross section calculation is assigned to be 0.10% [36]. The systematic uncertainty caused by MC statistics is estimated to be 0.05% according to the generated 5 million Bhabha MC events for each energy point.

To study the effect of $E_{\rm cms}$ uncertainty on the cross section calculation in the BabaYaga@NLO generator, the input values of $E_{\rm cms}$ are varied within 2 MeV, and the corresponding maximum change in the obtained cross section is taken as the systematic uncertainty.

As a cross check, the di-photon process is used to obtain the luminosity. To select the signal candidates, we require that there be at least two shower clusters in the EMC and no charged tracks detected in the MDC. The clusters must satisfy $|\cos\theta^{\rm EMC}| < 0.8$. To select back-to-back photon showers and reduce the backgrounds of Bhabha events, their angles with respect to the IP must be larger than 178°, and $\Delta\phi^{\rm EMC}$ of the two showers must be within $[-3°, 3°]$. To account for the EMC saturation effect and reduce the dimuon backgrounds, the hit number of one EMC shower must be larger than 20. These requirements are optimized based on the inclusive MC sample. The cross section and detection efficiency are determined by the BabaYaga@ NLO generator. Using Eq. (3), the resultant luminosity results at different energy points and the ratios between the measured luminosities based on the Bhabha and di-photon processes are consistent with unity, as shown in Table 1.

V. SUMMARY

The center-of-mass energies and integrated luminosities of e^+e^- annihilation data between 4.61 and 4.95 GeV collected from 2020 to 2021 by the BESIII detector at the BEPCII collider are measured with high precision. By adopting a novel method for analyzing $\Lambda_c^+\bar{\Lambda}_c^-$ pair-production in electron-position annihilations, the center-of-mass energies are measured with a precision of ~0.6 MeV, which is dominated by the precision of the known Λ_c mass. The integrated luminosities of the collected data samples are measured with a precision better than 1% by analyzing large-angle Bhabha scattering events after considering the EMC saturation effect. These results offer fundamental inputs for physics analyses based on these data samples.

ACKNOWLEDGEMENTS

The BESIII Collaboration thanks the staff of BEPCII and the IHEP computing center for their strong support.

References

[1] N. Brambilla, S. Eidelman, C. Hanhart *et al.*, Phys. Rept. **873**, 1-154 (2020)
[2] F. K. Guo, C. Hanhart, U. G. Meißner *et al.*, Rev. Mod. Phys. **90**, 015004 (2018)
[3] H. X. Chen, W. Chen, X. Liu *et al.*, Phys. Rept. **639**, 1-121 (2016)
[4] S. L. Olsen, T. Skwarnicki, and D. Zieminska, Rev. Mod. Phys. **90**, 015003 (2018)
[5] S. L. Olsen, Front. Phys. (Beijing) **10**, 121-154 (2015)
[6] N. Brambilla, S. Eidelman, B. K. Heltsley *et al.*, Eur. Phys. J. C **71**, 1534 (2011)
[7] M. Ablikim *et al.* (BESIII Collaboration), Phys. Rev. Lett. **126**, 102001 (2021)
[8] H. B. Li and X. R. Lyu, Natl. Sci. Rev. **8**, nwab181 (2021)
[9] M. Ablikim *et al.* (BESIII Collaboration), Phys. Rev. Lett. **116**(5), 052001 (2016)
[10] M. Ablikim *et al.* (BESIII Collaboration), Phys. Rev. Lett. **115**(22), 221805 (2015)
[11] M. Ablikim *et al.* (BESIII Collaboration), Phys. Rev. Lett. **121**(6), 062003 (2018)
[12] M. Ablikim *et al.* (BESIII Collaboration), Phys. Rev. Lett. **121**(25), 251801 (2018)
[13] M. Ablikim *et al.* (BESIII Collaboration), Phys. Rev. Lett. **120**(13), 132001 (2018)
[14] M. Ablikim *et al.* (BESIII Collaboration), Phys. Rev. D **103**(9), L091101 (2021)
[15] H. Y. Cheng, Chin. J. Phys. **78**, 324-362 (2022), arXiv:2109.01216 [hep-ph]
[16] E. V. Abakumova *et al.*, Nucl. Instrum. Meth. A **659**, 21-29 (2011)
[17] B. Wang, L. Y. Dong, and X. D. Ruan, Nuclear Electronics and Detection Technology, **33**, 240-244(2013).

https://kns.cnki.net/kcms/detail/detail.aspx?dbcode=CJFD&dbnameCJFD2013&filenam=HERE201302028&uniplatorm=NZKPT&vZDq7EQODJ6choXbFr3DRbj5vsa5ghdG0GsHdrnW6X0-ka7OKrq6Tk2G6ct25vmPC
[18] M. Ablikim *et al*. (BESIII Collaboration), Nucl. Instrum. Meth. A **614**, 345-399 (2010)
[19] C. H. Yu *et al*., IPAC2016 Proccedings, (2016)
[20] M. Ablikim *et al*. (BESIII Collaboration), Chin. Phys. C **44**, 040001 (2020)
[21] X. Li *et al*.,, Radiat. Detect. Technol. Methods **1**, 13 (2017)
[22] Y. X. Guo *et al*.,, Radiat. Detect. Technol. Methods **1**, 15 (2017)
[23] P. Cao *et al*.,, Nucl. Instrum. Meth. A **953**, 163053 (2020)
[24] S. Agostinelli *et al*. (GEANT4 Collaboration), Nucl. Instrum. Meth. A **506**, 250 (2003)
[25] S. Jadach, B. F. L. Ward, and Z. Was,, Phys. Rev. D **63**, 113009 (2001)
[26] S. Jadach, B. F. L. Ward, and Z. Was, Comput. Phys. Commun. **130**, 260 (2000)
[27] D. J. Lange, Nucl. Instrum. Meth. A **462**, 152 (2001)
[28] R. G. Ping, Chin. Phys. C **32**, 599 (2008)
[29] P. A. Zyla *et al*. (Particle Data Group), PTEP **2020**, 083C01 (2020)
[30] J. C. Chen, G. S. Huang, X. R. Qi et al,, Phys. Rev. D **62**, 034003 (2000)
[31] R. L. Yang, R. G. Ping, and H. Chen, Chin. Phys. Lett. **31**, 061301 (2014)
[32] E. Richter-Was, Phys. Lett. B **303**, 163 (1993)
[33] B. Aubert *et al*. (BaBar Collaboration), Phys. Rev. D **72**, 052006 (2005)
[34] A. D. Bukin, Fitting function for asymmetric peaks, arXiv: 0711.4449
[35] M. Ablikim *et al*. (BESIII Collaboration), Phys. Rev. Lett. **112**, 132001 (2014)
[36] G. Balossini, C. Bignamini, C. M. C. Calame *et al*., Phys. Lett. B **663**, 209-213 (2008)
[37] M. Ablikim et al (BESIII Collaboration), arXiv: 2203.03133[hep-ex]